Supplementary Information for "High-Speed Limnology: Using Advanced Sensors to Investigate Spatial Variability in Biogeochemistry and Hydrology"

John T. Crawford*[1,2], Luke C. Loken[2], Nora J. Casson[2,3], Colin Smith[2], Amanda G. Stone[2], and Luke A.Winslow[2,4]

1: U.S. Geological Survey, National Research Program, 3215 Marine St., Boulder, CO, 80303, USA *corresponding author

2: University of Wisconsin-Madison, Center for Limnology, 680 N. Park St. Madison, WI, 53706, USA

3: Present Address: University of Winnipeg, Department of Geography, 515 Portage Ave. Winnipeg, Manitoba, Canada

4: Present Address: U.S. Geological Survey, Center for Integrated Data Analytics, Middleton, WI, 53562, USA

This supplementary file contains 31 pages, three tables and five figures.

Intake Manifold

A component list and assembly diagram for the FLAMe intake manifold are given in Table S1 and Figure S1. Our design requires welding of threaded nuts for set screws on the high-speed intake, welding a pipe elbow to the bottom of the high-speed intake, and welding of flat bars to C-clamps in order to secure the manifold to the boat. Other parts can be attached with simple hand tools. Threaded pipe components are sealed with Teflon tape, and non-threaded pipes are joined and sealed with PVC cement. The high-speed reservoir is constructed of clear plastic pipe to allow flow monitoring. The mechanical gas equilibrator was also constructed from clear plastic pipe to allow observation of the full-cone sprayer nozzle. The sprayer head is a plastic 3/8" full-cone spray nozzle connected to straight PVC pipe. The equilibration chamber has inlet and outlet ports that are connected to an external gas analyzer (discussed below). The outlet of the equilibrator chamber is similar to the design of a household plumbing trap which prevents gas moving back into the chamber. This design allows the water volume in the trap to create a headspace in the chamber that is closed to the atmosphere.

Sensor Control Box

We constructed a control box to direct water flow to the sensors (Figure S2). Two electrically controlled, three-way ball valves were used to select from the three inlet sources: 1) slow-speed intake, 2) high-speed intake, 3) onboard reservoir (charge tank). The onboard reservoir can be used for system priming (if needed), system flushing, or system response experiments using tracers such as KCl for conductivity (discussed below). One ball valve selects between the high-speed and slow-speed intake, whereas the other toggles between the reservoir and the selected intake port. Once water is routed into the box and through the valve system, it is

drawn through the sensor flow-through cells, and then into a DC impeller pump. Water is then pumped out of the box and through the equilibrator nozzle. We also included a "Y" junction upstream of the pump that was connected to a DC peristaltic pump which was used for discrete water sampling. The pumps and valves are all controlled by a switch board that can be mounted internally or externally. The system is powered by a minimum of two 12 V batteries wired in parallel. We chose to mount the batteries in a separate box to prevent possible exposure to water.

We solved for the water residence time (τ_w, s) of the system using Equation 1

$$\tau_w = V / q \quad \text{(Equation 1)}$$

where V is the volume of the system (L) and q is the flow rate of the system (L s^{-1}). We estimated q from triplicate measurements of outlet flow, and then determined V by first fully priming the system with water from the slow-speed intake and then flushing all of the water into a graduated cylinder using compressed air. Our design had an average τ_w of 33 seconds.

Sensor response experiments

We conducted a series of sensor response experiments on Lake Mendota on August 1, 2014. The goal was to understand the potential lags and minimum response times for the EXO2 and UGGA sensors integrated into the FLAMe platform. These data were then used to develop correction procedures for higher accuracy spatial datasets. To test sensor responses to step-changes in water chemistry, we mixed a 40 L tracer solution into a plastic carboy that was connected to the reservoir port on the FLAMe. The reservoir was mixed with 50 mL of rhodamine WT to test the phytoplankton fluorescence sensors, 6 mL of quinine sulfate solution in acid buffer (100 QSE) to test the fDOM sensor, 14 g of KCl to test the conductivity sensor, and ~2 kg of ice to reduce the temperature of the solution relative to lake water. The mixture

volume was increased to 40 L using tap water. We did not modify the CO_2 concentration or pH in the carboy as we found the municipal water source to have greater than ambient lake CO_2 (4300 vs. 290 µatm, respectively) and lower pH (7.5 vs 8.3, respectively). A comparison of initial readings from the carboy and average readings from Lake Mendota are given in Table S2. At the beginning of the experiments, we allowed lake water to circulate through the system for ~10 minutes. We then switched to the tracer solution for a period of five minutes, followed by five minutes of lake water, then back to the tracer solution for an additional five minutes. The goal was to reach steady-state plateau readings from each sensor. Following the plateau experiments we ran two sequences of discrete reservoir pulses through the FLAMe in ascending intervals (5, 10, 20, 30 and 60 seconds).

The results of both experiments for CO_2, pH, conductivity and temperature are shown in Figure S3. Of these four sensors, we found that conductivity, temperature and pH from the EXO2 responded immediately, and reached plateau within 60 seconds. The UGGA responded slower, but CO_2 still reached plateau within 120 seconds. The experimental results for the optical sensors are shown in Figure S4. Similar to the other EXO2 parameters, most of the optical sensors responded rapidly and reached a plateau concentration during the experiment. Turbidity and dissolved oxygen responded fastest, whereas chlorophyll-*a* and fDOM responded slower. The fDOM sensor did not reach steady state during either of the five minute experiments, which we predict was a result of changing pH conditions and thus fluorescent yield of the quinine sulfate in the carboy. However, this unclear result does not indicate that the sensor is incapable of rapid response to changing organic matter concentrations and composition. Future sensor response experiments should therefore be conducted with a natural organic matter source under more stable temperature and pH conditions.

The pulse experiments support the findings from the plateau data (Figures S3 and S4). In general, the sensors approached plateau concentrations within 60 seconds, while some reached similar levels in as little as 30 seconds (approximately equal to τ_w). Although we repeated the pulse experiments with the same source of tracer as the plateau experiments, they are not directly comparable for all parameters. For example, we observed a steady temperature rise in the reservoir during the experiment because the carboy was in direct sunlight. Similarly, CO_2 decreased and pH increased over the course of the afternoon presumably due to degasing from the carboy.

Using the step-change experiment data, we determined each sensor's hydraulic time constant (H_r) and parameter time constant (τ_s). The sensor-specific H_r is a function of system water residence time and sensor position/shielding within the system. τ_s is the time required for a 63% response to a step-change input. H_r was calculated based on the plateau experiments and was indicated by the first observation with a non-zero rate of change. All EXO2 sensors had $H_r <$ 12 s, and most had responses less than 5 s (Table S3). The CO_2 sensor had a much greater H_r than the EXO2 sensors because water must travel further through the system before equilibrating with the gas solution being pumped to the UGGA. On average it took 22 s for the CO_2 sensor to detect a change in the intake water. Using these H_r values, we offset response variables thus removing the hydraulic lag (Figure S5). However, this correction does not account for sensor-specific response patterns (τ_s). The EXO2 sensors have manufacturer-reported τ_s values between 2-5 s, but these values are not appropriate to apply to the FLAMe system because they do not include system hydraulic lag and mixing. In order to match sensor readings with spatial information, we first applied H_r values from each sensor output according to equation 2. This

step aligns the time at which each sensor begins responding to the changing water, and accounts for the physical distance the water must travel before being sensed

$$X_{t-Hr} = X_c \quad \text{(Equation 2)}$$

Where X_c is the hydraulic-corrected sensor output at time *t* and X_{t-Hr} is the sensor output at time *t* minus H_r

In order to match individual sensor response characteristics and to obtain more accurate spatial data, we then applied sensor-specific corrections using Equation 3 (Fofonoff et al., 1974).

$$X_o = X_c + \tau_s \frac{dX}{dt} \quad \text{(Equation 3)}$$

where X_o is the τ_s-corrected value at time *t* and $\frac{dX}{dt}$ is the instantaneous rate of change of sensor output. We first smoothed the raw data using a running mean of 3 observations in order to reduce inherent noise of the 1 Hz data. We then calculated $\frac{dX}{dt}$ using a 3-point moving window around X_c. Equation 3 should ideally lead to a step response to a step-change input. We note that this is the same strategy used to correct oceanographic conductivity and temperature instruments (see Fozdar et al., 1985). Three examples of smoothed data using the H_r and τ_s corrections are provided in Figure S5. Overall, the τ_s-corrected data show good responses to step-change inputs and indicate that this is a useful technique for generating higher accuracy spatial data.

Supplementary References

Fofonoff N.P., Hayes S.P., and Millard Jr. R.C. (1974). W.H.O.I./Brown CTD microprofiler: Methods of calibration and data handling. WHOI Tech. Rep. WHOI-74-89.

Fozdar F.M., Parker G.J., and Imberger J. (1985). Matching temperature and conductivity sensor response characteristics. *Journal of Physical Oceanography,* 15: 1557–1569.

Supplementary Information Tables

Table S1: Parts list for intake manifold corresponding to Figure S1

Item	Description	Quantity	notes
1	Bar, Flat (6 x 25 x 100 mm, steel)	8	Welded inside of items 28 and 29 to accomodate fitting of items 17 and 18.
2	Bar, Flat (6 x 44 x 64 mm, steel)	2	Holes (x2) drilled for OD of item 26. Welded to screw swivel of item 6.
3	Bar, Flat (6 x 44 x 240 mm, steel)	2	Bent 90 degrees and welded to items 6, 28 and 29.
4	Block (19 x 44 x 64 mm, wood)	2	Joined to item 2 with items 26 and 30.
5	Bolt (M10 x 1.5 x 25 mm, steel)	4	Threads to item 12. Acts as set screw for height adjustment of items 17 and 18.
6	Clamp, 'C' (0 - 203 mm opening, 114 mm reach, steel)	2	Welded to items 2 and 3. Clamps to boat transom. Opening and reach should accomodate boat.
7	Clamp, Hose (12.7 mm band, size 89 -140 mm, stainless)	2	Joins gas equilibrator to fast intake pipe.
8	Hose Adapter, Barbed (1/4" BSPT male to 1/4", acetal)	2	Threaded to item 15 with teflon tape.
9	Hose Adapter, Barbed (3/8" BSPT male to 3/8", acetal)	2	Threaded to items 14 and 25 with teflon tape.
10	Hose Adapter, Barbed (1/2" BSPT male to 3/8", brass)	1	Threaded to item 17 with teflon tape.
11	Nozzle, Sprayer (3/8" BSPT male, full-cone spray, brass)	1	Threaded to item 25 with teflon tape. Maximum flow rate 78 lpm @ 27 bar.
12	Nut (M10 x 1.5 x 10 mm, steel)	4	Welded to items 28 and 29 centered over drilled holes.
13	Pipe (50 mm, heavy, length = 45 mm, PVC)	4	Joined and sealed with PVC cement.
14	Pipe (50 mm, heavy, length = 150 mm, PVC clear)	1	3/8" BSPT threaded hole added. Joined and sealed with PVC cement.

15	Pipe (50 mm, heavy, length = 260 mm, PVC clear)	1	1/4" BSPT threaded holes (x2) added. Joined and sealed with PVC cement to item 24. Do not use PVC cement when joining item 20.
16	Pipe (50 mm, heavy, length = 175 mm, PVC)	2	Joined and sealed with PVC cement.
17	Pipe (DN 15 mm, seamless, heavy, length = 480 mm, 1/2" BSPT male to 1/2" BSPT female, galvanized steel)	1	Threads to items 10 and 21 with teflon tape.
18	Pipe (DN 15 mm, seamless, heavy, length = 1080 mm, 1/2" BSPT male to 1/2" BSPT male, galvanized steel)	1	Threads to item 22 (x2) with teflon tape. Item 22 at base of item 18 is welded to fix orientation forward to the boats bow.
19	Pipe (DN 20 mm, seamless, heavy, length = 115 mm, 3/4" BSPT male to 3/4" BSPT male, galvanized steel)	1	Threads to items 20 and 23 with teflon tape.
20	Pipe Cap (50 mm, heavy, PVC)	2	3/4" BSPT threaded hole added to item 20 joining with item 19. 27 mm hole drilled added to item 20 joined to item 15, which is not sealed to item 15 with PVC cement.
21	Pipe Coupling (1/2" BSPT female to 1/2" BSPT female, galvanized steel)	1	Welded to item 27.
22	Pipe Elbow (1/2" BSPT female to 3/4" BSPT female, galvanized steel)	2	Threaded to items 18 and 23 with teflon tape. Welded to base of item 18.
23	Pipe Elbow (3/4" BSPT male to 3/4" BSPT female, steel)	1	Threaded to items 19 and 22 with teflon tape.
24	Pipe Elbow (50 mm, heavy, PVC)	6	Joined and sealed with PVC cement.
25	Pipe Through-wall Fitting (3/8" BSPT female to 3/8" BSPT female, EPDM gasket, PVC)	1	Is two parts (25a and 25b) Threaded to items 9 and 11 with teflon tape. Joined and sealed to item 20.
26	Screw (M3.9 x 13, steel)	4	Joins items 2, 4 and 30.
27	Screen (2 mm mesh, steel)	1	Welded to item 21.

28	Tube, Square (40 x 3.2 mm x 400 mm, steel)	1	Holes (x2) drilled for OD of item 5. Item 12 (x2) is welded over holes. Item 1 (x4) is welded inside top and bottom of tube.
29	Tube, Square (40 x 3.2 x 500 mm, steel)	1	Holes (x2) drilled for OD of item 5. Item 12 (x2) is welded over holes. Item 1 (x4) is welded inside top and bottom of tube.
30	Washer (M4, steel)	4	Joined with item 26.

Table S2: Lake and initial carboy water chemistry measured independently during sensor response experiments

Parameter	Carboy Water	Lake Water
Water Temperature (C)	12.93	23.84
Specific Conductivity (µS cm^{-1})	1249	509
pH	7.51	8.72
Dissolved Oxygen (mg L^{-1})	7.76	11.25
Dissolved Oxygen (% saturation)	73.8	133.6
pCO_2 (µatm)	4050	290

Table S3. Hydraulic response times (H_r) and sensor time constants (τ_s) (both in seconds) for FLAMe water chemistry parameters; all values are the mean of 4 replicate step-change inputs (± standard deviations)

Instrument	**Sensor**	H_r	τ_s
YSI-EXO2	pH	2.8 ± 2.2	6.8 ± 1.5
YSI-EXO2	Specific Conductivity	3.0 ± 1.4	7.5 ± 1.3
YSI-EXO2	Temperature	4.0 ± 2.7	9.3 ± 1.3
YSI-EXO2	fDOM	5.5 ± 3.7	7.5 ± 8.7
YSI-EXO2	Turbidity	8.25 ± 6.0	12.2 ± 3.2
YSI-EXO2	Dissolved Oxygen	4.3 ± 3.2	14.8 ± 3.3
YSI-EXO2	Chlorophyll-*a*	11 ± 12	15.8 ± 7.3
UGGA	CO_2	22 ± 4.9	35.2 ± 7.4

Supplementary Information Figures

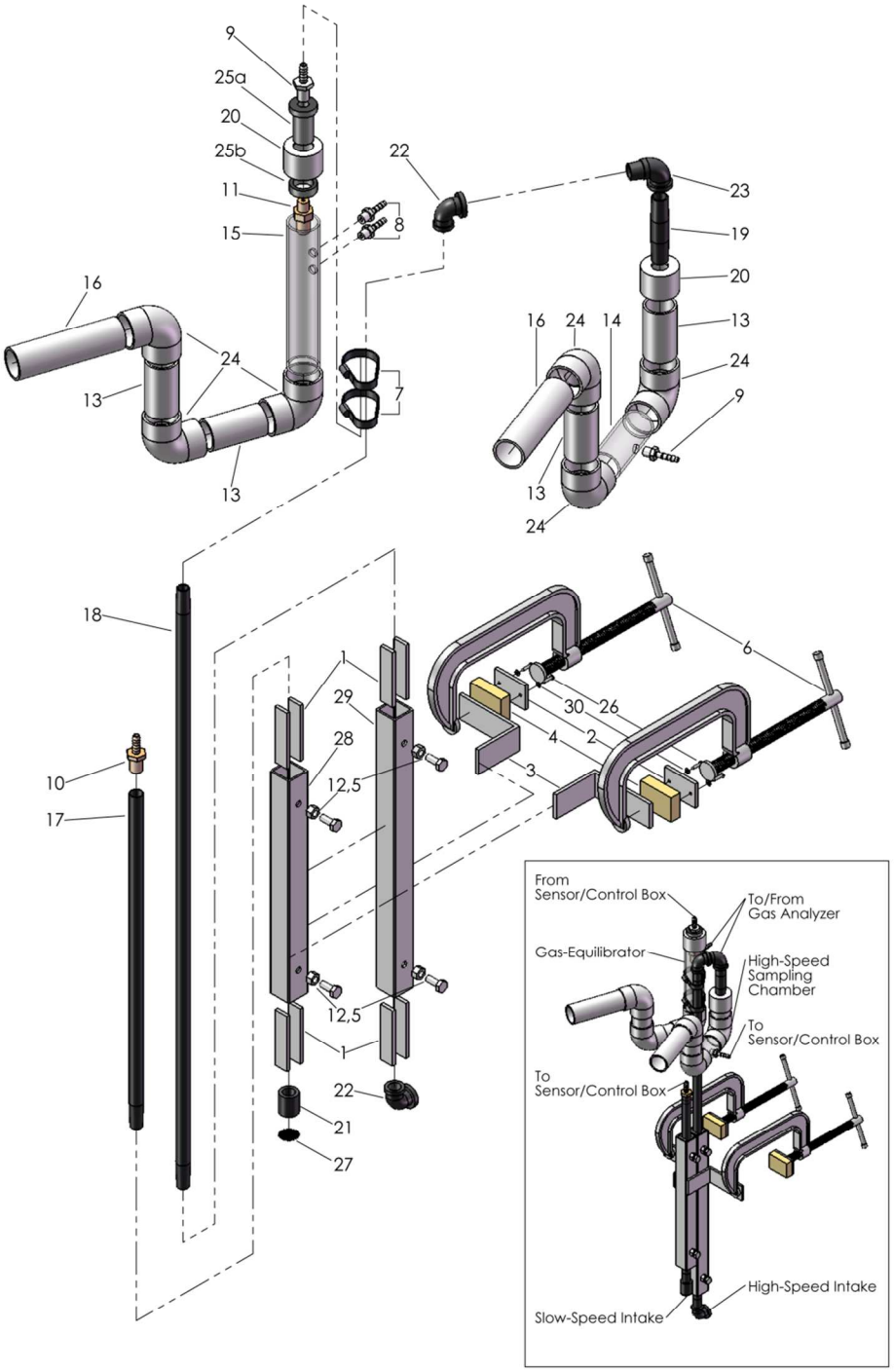

Figure S1: Computer rendering (exploded view) of the FLAMe water intake with part numbers corresponding to Table S1

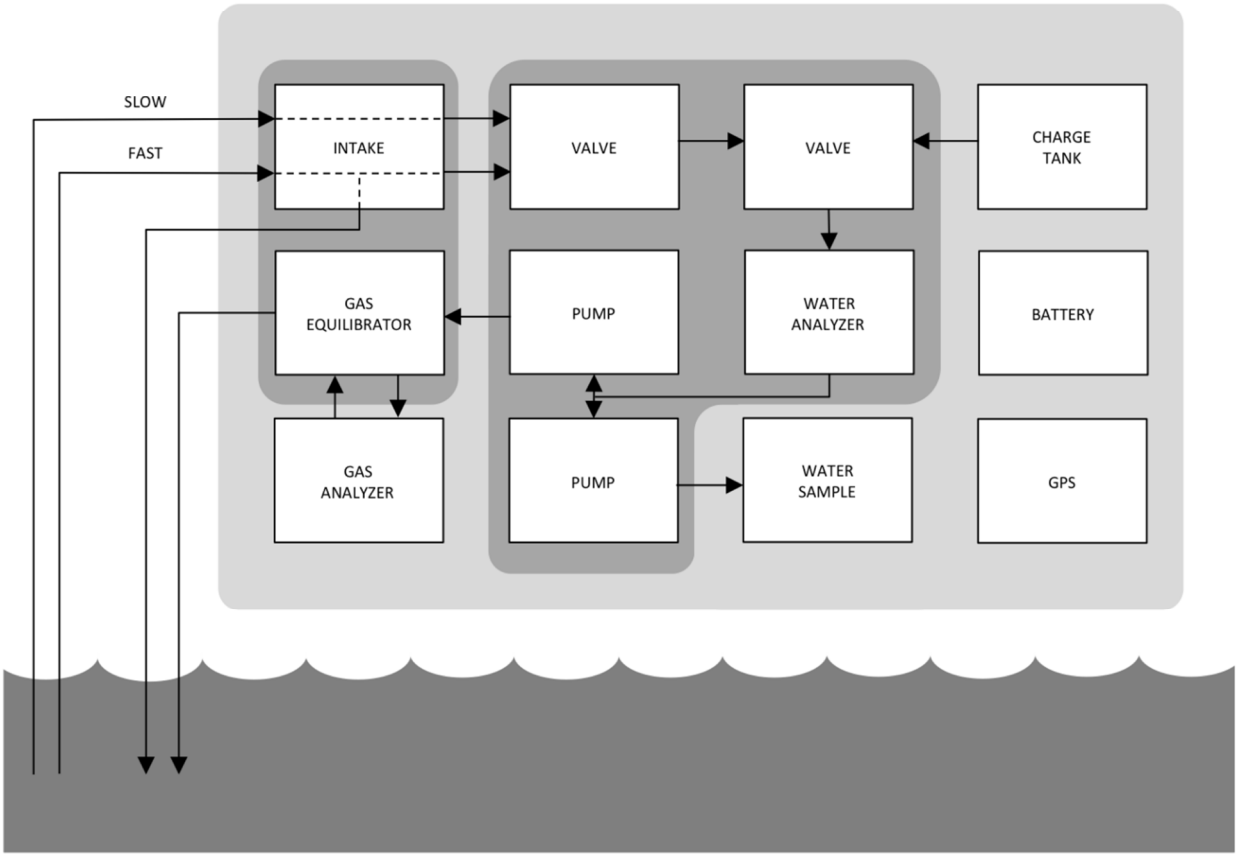

Figure S2: Diagram of the FLAMe control box

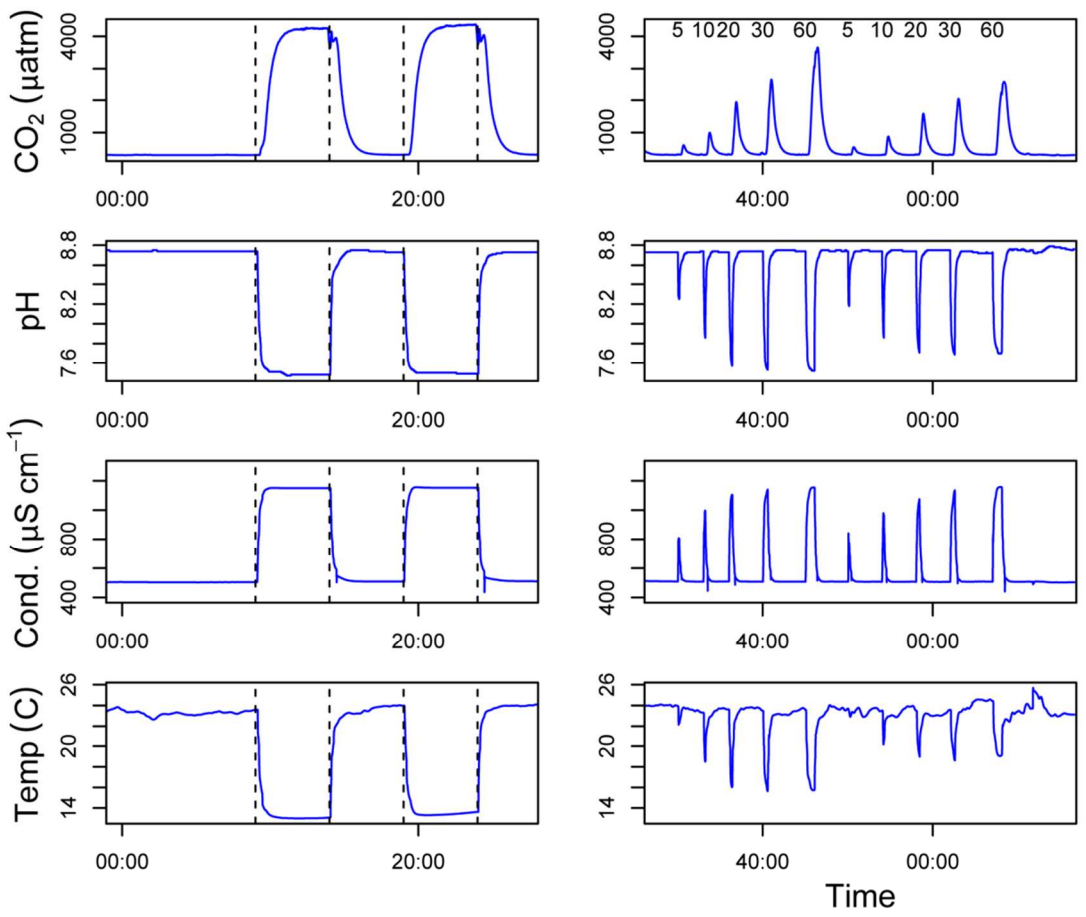

Figure S3: Plateau and pulse input results from Lake Mendota sensor response experiment (basic sensors)

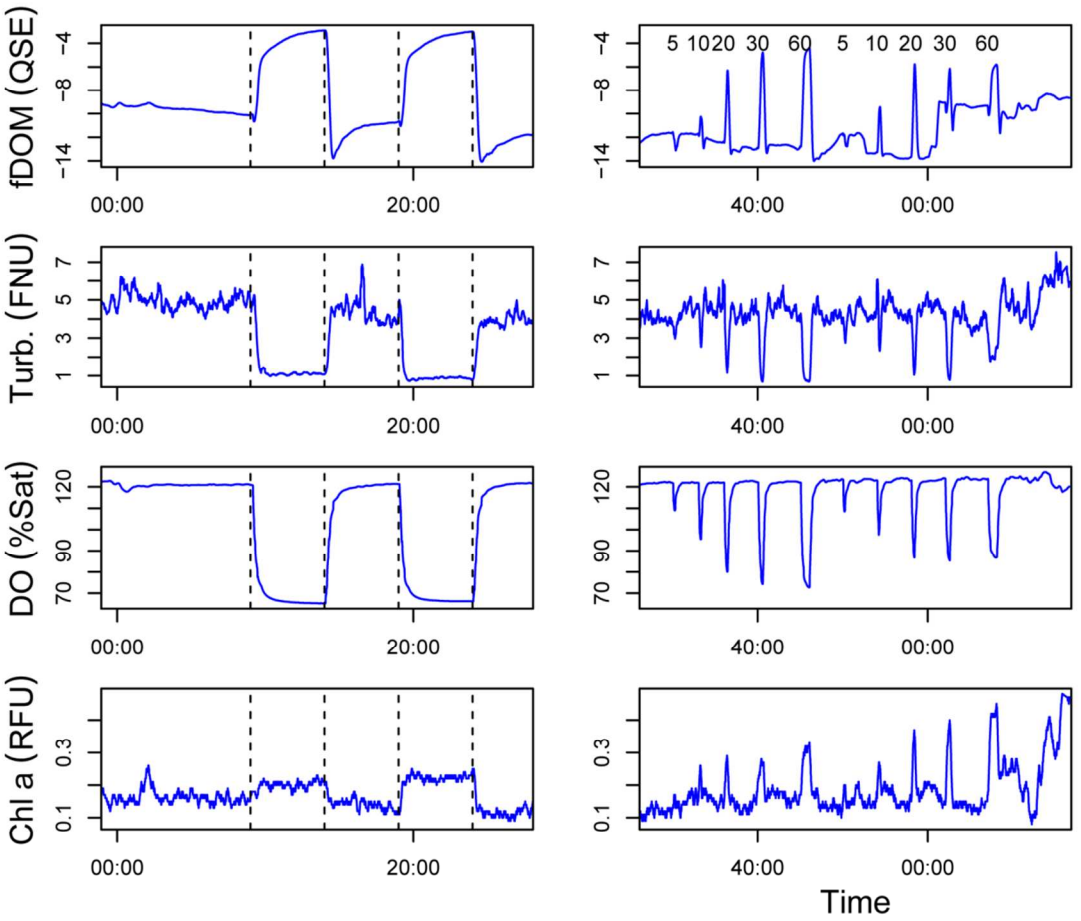

Figure S4: Plateau and pulse input results from Lake Mendota sensor response experiment (optical sensors)

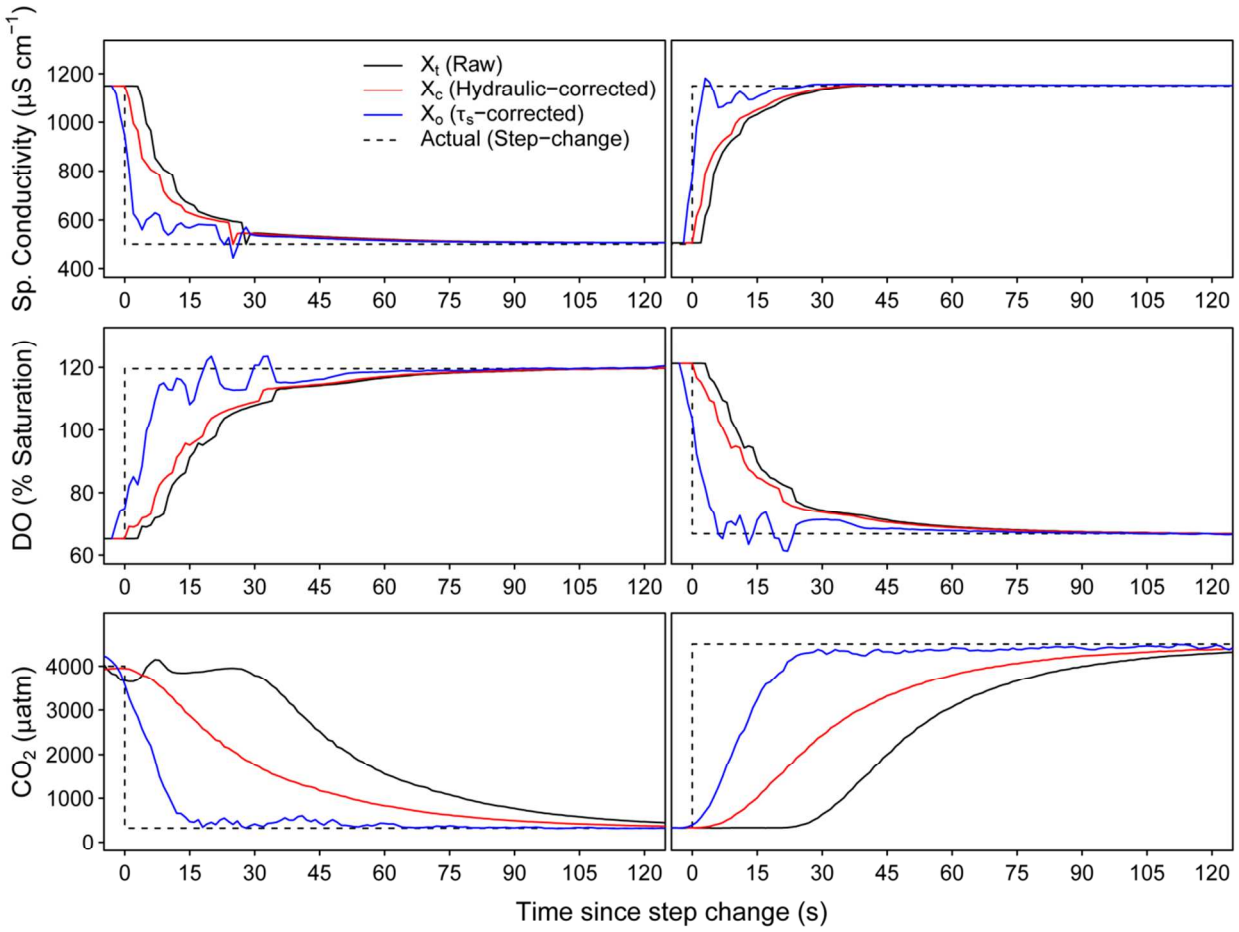

Figure S5: Raw data, hydraulic lag (R_h) corrected, and time constant (τ_s) reconstructed sensor response curves from step-change inputs